Available online at www.sciencedirect.com
ScienceDirect
Trans. Nonferrous Met. Soc. China 23(2013) 3353−3361
Transactions of Nonferrous Metals Society of China
www.tnmsc.cn

Molecular dynamics study on temperature and strain rate dependences of mechanical tensile properties of ultrathin nickel nanowires

Wei-dong WANG, Cheng-long YI, Kang-qi FAN

School of Electrical and Mechanical Engineering, Xidian University, Xi'an 710071, China

Received 25 September 2012; accepted 29 April 2013

Abstract: Based on the EAM potential, a molecular dynamics study on the tensile properties of ultrathin nickel nanowires in the ⟨100⟩ orientation with diameters of 3.94, 4.95 and 5.99 nm was presented at different temperatures and strain rates. The temperature and strain rate dependences of tensile properties were investigated. The simulation results show that the elastic modulus and the yield strength are gradually decreasing with the increase of temperature, while with the increase of the strain rate, the stress—strain curves fluctuate more intensely and the ultrathin nickel nanowires rupture at one smaller and smaller strain. At an ideal temperature of 0.01 K, the yield strength of the nanowires drops rapidly with the increase of strain rate, and at other temperatures the strain rate has a little influence on the elastic modulus and the yield strength. Finally, the effects of size on the tensile properties of ultrathin nickel nanowires were briefly discussed.

Key words: ultrathin nickel nanowires; temperature dependence; strain rate dependence; tensile properties; molecular dynamics simulation

1 Introduction

In recent years, many researchers have paid more attention on the nanomaterials due to their unique mechanical, electrical, optical and other properties. Recently an explosive interest has accrued in one-dimensional nanostructures [1,2]. As one of the typical nanomaterials, the metal nanowires have broad application prospects [3,4] in nanoprobe, nanoelectro-mechanical systems (NEMS) and biomedical fields, and are expected to play an important role in future research. Many difficulties including the theoretical prediction methods of mechanical properties, the synthesis methods of these nanostructures and the experimental approaches, are still remaining on the road of applications of one-dimensional nanostructures, such as metallic or non-metalic nanowires, nanotubes.

Metallic nanowires have received considerable attention recently, especially in numerical simulation studies [5]. The mechanical properties of the metal nanowires are important factors that have effects on their applications and reliabilities. WU et al [6] studied the tensile strength and fracture of copper nanowires under uniaxial tension, and found that the strength of copper nanowires is much larger than that of the bulk copper, and the cross-sectional size of the nanowires and the tensile strain rate affect the yield strength and the mechanical deformation. DIAO et al [7,8] analyzed the strength of gold nanowires with the method of molecular dynamics simulation. PARK et al [9,10] and LIANG and ZHOU [11] simulated the uniaxial tension of gold and copper nanowires, and observed the shape memory effect and pseudo-elastic behavior of the nanowires. KOH et al [12] simulated the temperature dependence and strain-rate dependence of the deformation characteristics and mechanical properties of the platinum nanowires under unidirectional uniform tensile, and pointed out that under the conditions of low temperature and low strain rate, the stress—strain curves of platinum nanowires show a stepped cycle distribution, and the nanowire maintains ordered and stable crystal structure at this time. PARK et al [13] simulated axial tension and compression of copper, gold, and nickel nanowire in its ⟨100⟩ and

Foundation item: Project (51205302) supported by the National Natural Science Foundation of China; Project (2013JM7017) supported by the Natural Science Basic Research Plan in Shanxi Province of China; Project (K5051304006) supported by the Fundamental Research Funds for the Central Universities, China

Corresponding author: Wei-dong WANG; Tel: +86-29-88201974; E-mail: wangwd@mail.xidian.edu.cn

DOI: 10.1016/S1003-6326(13)62875-7

⟨110⟩ crystal orientations, indicating that the mechanical deformation of the nanowires was the inherent property of the material. ZHANG et al [14,15] studied the structure and properties of the nickel nanowires with the initial configuration of FCC structure when compressed in the axial direction, using the generalized simulated annealing method with Sutton Chell potential, and drew a conclusion that radial compression level affected the structure of the nickel nanowires greatly. GARCÍA-MOCHALES et al [16,17] focused on the influence of the tensile direction and temperature on the nickel configuration, and uncovered the findings that the nickel nanowire appeared a minimum cross-section with 5 atoms, and the formation was enhanced if the temperature was raised to 500 K, but at higher temperature, the configuration declines. SETOODEH et al [18], HUANG et al [19], and WEN et al [20,21] studied the mechanical properties of nickel stretched in axial direction impacted by the strain rate and the size of the nanowires using the method of molecular dynamics simulation. SANSOZ and DUPONT [22] studied the nanoindentation and plasticity properties of nickel nanowires in nanocrystalline.

Except for the above numerical studies, there are a few experimental efforts on mechanical properties of metallic nanowires. ZHENG et al [23] and LU et al [24,25] directly observed the deformation and fracture mechanisms of gold nanowires below sub-20 nm range through experiments. Limited by the existing experimental conditions and technical means, it is very difficult to study the metal nanowires in direct ways. However, analysis of the metal nanowires in the method of molecular dynamics simulation is an effective way at nanoscale [26]. Although some research has been done on the tensile properties of ultrathin nickel nanowires in the above mentioned, the variation of stress—strain has not yet reached a consensus, and rarely involves the study of the temperature dependence. The temperature and strain-rate dependence of the tensile properties of metal nanowires is an important element in nanotechnology research, and the microstructure of nanowires is not easy to precisely control, therefore the tensile properties of ultrathin nickel nanowires are investigated at a wide range of thermodynamic temperature and different strain rates based on molecular dynamics method.

2 Physical modeling and molecular dynamics simulation

The lattice for the perfect single-crystal nickel nanowire is in the form of FCC structure, and here the lattice parameter of bulk nickel is utilized, 3.524 Å (300 K). Three nickel nanowire models with the same length of 15 nm and different diameters of 4, 5, and 6 nm, respectively, are built in this work. Considering the modeling errors with the LAMMPS software, the real diameters are 3.94, 4.95 and 5.99nm, respectively. The axial direction of nickel nanowires model is the ⟨100⟩ crystallographic orientation of FCC lattices, in which the periodic boundary condition is applied, and the non-periodic boundary conditions is applied in other orientations (⟨010⟩ and ⟨001⟩).

This work utilizes embedded atom method (EAM) potential [27,28] to describe the interactions between the nickel atoms in molecular dynamics simulation. EAM potential is a kind of N-body potential that reflects the interactions between atoms as well as the corresponding anisotropic. The total potential energy of the crystal is divided into two parts: one part of the energy is pair potential between the atoms in the crystal lattice; the other is the embedded energy of atoms embedded in the electron cloud background, and it represents the many-body interactions. The pair potential and embedded potential that form the EAM potential are selected in accordance with the experience. For the EAM potential, the total potential energy of the crystal can be expressed as

$$U=\sum_i F_i(\rho)+\frac{1}{2}\sum_{j\neq i}\phi_{ij}(r_{ij}) \tag{1}$$

where $\sum_i F_i(\rho)$ is embedded energy; $\frac{1}{2}\sum_{j\neq i}\phi_{ij}(r_{ij})$ is pair potential, which can be selected according to the needs of the different forms; ρ is the summation of electron cloud density generated by all other atoms extranuclear except the i-th atom in the position of i-th atom, which can be expressed as

$$\rho=\sum_{j\neq i} f_j(r_{ij}) \tag{2}$$

where $f_j(r_{ij})$ is the charge density that the j-th atom extranuclear contribute in the position of the i-th atom; r_{ij} is the distance between the i-th atom and the j-th atoms. For different metals, the embedded potential function and the pair potential function can be determined by fitting the metal macroscopic parameters.

System balance is one of the basic requirements for MD simulations. Before performing any MD simulations, one should firstly allow the system freely evolve to its balance state without imposing any external force on the ideal model. During the MD simulations, the time step is set as 1 fs, and the NVT ensemble is utilized. In order to study the temperature effects on the tensile properties of nickel nanowires, the system temperatures are set as 0.01, 300, 600, 900, 1200, 1500 and 1800 K respectively in MD simulations.

Another important requirement for MD simulations

is sufficient relaxation. For all of models in this work, the atomic configuration and the total system energy are basically stable after an about 50 ps relaxation process, that is to say, the system is in a fully relaxed state. This atomic configuration at this moment is taken as the initial state. Then, the nanowires are stretched in the axial direction, i.e. ⟨100⟩ crystal orientation. According to the existing Refs. [18,20,21], most of stretching speeds range from 10 to 1000 m/s. In this work, four stretching speeds are selected to perform tensile simulations, including 20, 80, 140 and 200 m/s, and the corresponding strain rates shown in Table 1 are 1.384×10^9, 5.536×10^9, 9.688×10^9 and 1.384×10^{10} s^{-1}, respectively.

Table 1 Strain rates versus stretching speeds

Strain rate/s^{-1}	Stretching speed/(m·s^{-1})
1.384×10^9	20
5.536×10^9	80
9.688×10^9	140
1.384×10^{10}	200

3 Simulation results and discussion

3.1 Stretching process

Figure 1 shows the nanowire morphology during the stretching process of the *d*4.95 nm nickel nanowire at the temperature of 300 K and strain rate of 1.384×10^{10} s^{-1}. According to the theoretical FCC structures, the original nanowire model is built as shown in Fig. 1(a). After being fully relaxed, the system reaches an energy minimum state, called initial state, and the atomic configuration is shown in Fig. 1(b). It can be found that the nanowire morphology is substantially consistent with the original theoretical model. Only after sufficient relaxation, some of the nickel atoms on the nanowire's surface are rearranged, resulting in some local lattice defects.

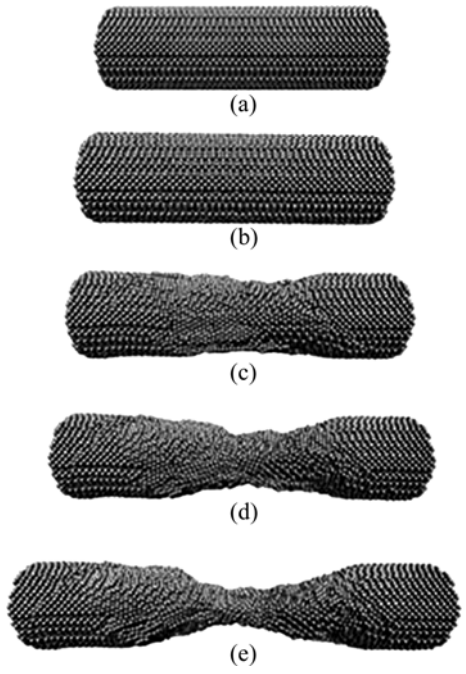

Fig. 1 Nanowire morphologies of *d*4.95 nm nickel nanowire at 300 K and strain rate of 1.384×10^{10} s^{-1} during stretching processes: (a) Original state; (b) Initial state, ε=0; (c) Yielding state, ε=0.10; (d) After yielding state; ε=0.18; (e) After yielding state, ε=0.30

During each MD simulation, the left end of the nanowire is fixed and the right one is applied the axial load at the strain rate of 1.384×10^{10} s^{-1}. With the increasing of the strain, the stress on the nanowire is basically linear increasing, which will be discussed in detail in the Section 3.3. When the strain ε is about 0.10, the nanowire takes on a yielding state, whose morphology is shown in Fig. 1(c). It can be seen that the nanowire's surface is cracked abruptly and some lattices slide on the cracking area at the moment, which results in a large number of lattice defects. Figures 1(d)−(e) show the nanowire morphologies after yielding state at the strain of 0.18 and 0.3, respectively.

Figure 2 shows the atomic configuration on the middle cross section of *d*4.95 nm nanowire. As shown in Fig. 2, before yielding, the nanowire keeps its original lattices; at the yielding state, a large number of lattice defects suddenly emerge inside the nanowire, and the stress at this state is called yield strength. As stretching going on, the lattice defects gradually increase and expand from the middle part to both ends of the nanowire, which results in the necking shape as shown in Figs. 1(d)−(e) and final rupture at the strain of 0.36.

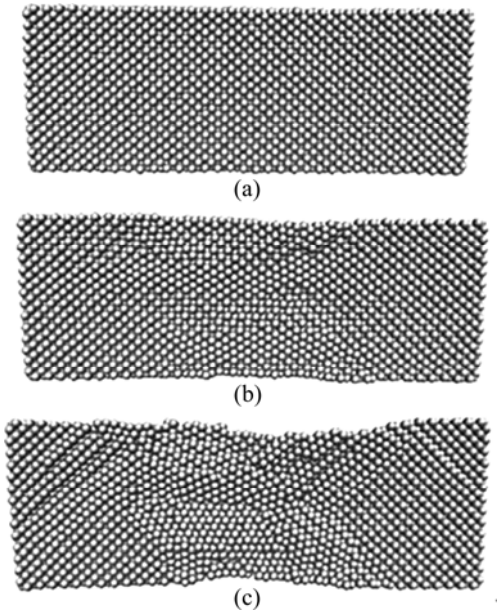

Fig. 2 Atomic configuration on middle cross section of *d*4.95 nm nanowire at 300 K and strain rate of 1.384×10^{10} s^{-1}: (a) Before yielding state; (b) Yielding state; (c) After yielding state

3.2 Simulation results and tensile properties

Through numerical MD simulations for these ultrathin nickel nanowires (*d*3.94 nm, *d*4.95 nm and *d*5.99 nm), the stress — strain curves have similar variation tendencies, except for some numerical distinctions. Herein, the *d*4.95 nm nanowire is taken as an instance to present the simulation results at different temperatures and different strain rates, as shown in Fig. 3.

It can be seen from Fig. 3 that all of the nanowires experience some similar stretching processes: elastic stretching, yielding state, plastic stretching and fracture. Before the yielding state, the nanowire is stretched linearly basically and the slope of the stress—strain curve is named elastic modulus. While at the yielding state, many lattice defects occur inside the nanowire, and the stress obtained by the nanowire reaches a maximum value named yield strength. Subsequently, with the strain's increasing, the stress abruptly decline and then the nanowire enters into a plastic deformation stage, i.e. the period of plastic stretching. During the period of plastic stretching, the stress received by the nanowire continuous decreases until fracture.

The above phenomena are mainly due to the different deformation mechanisms. Before the yielding state, the nanowire is in the elastic stretching stage. At this moment, few lattice defects and few atomic dislocations appear. As the nanowire is stretched, the distance between atoms increases, but still retains the original FCC lattice of nickel. While at yielding state, a number of lattice defects appear and the atomic arrangement is chaotic, plastic stretching and fracture followed.

Tables 2 and 3 list the tensile properties of elastic modulus and yield strength, respectively, for the ultrathin nanowires under different conditions. The elastic modulus reaches the maximum value of 134.7 GPa at 0.01 K, and the minimum value of 32.0 GPa at 1500 K. At the strain rate of 1.384×10^{9} s^{-1}, the greatest yield strength is 14.8 GPa at 0.01 K, while the weakest one is 1.8 GPa at 1500 K.

It can be concluded from Table 2 that with the increasing of temperature, the elastic moduli are constantly reduced for all cases of diameters. The yield strengths have the same trend on temperature. At 300 K, the elastic moduli are all 116−119 GPa. The yield strength at 300 K are all 11−12 GPa.

3.3 Results analysis

3.3.1 Dependence on temperature

From Fig. 3(a), it can be found that the elastic modulus and yield strength of nanowires decrease with

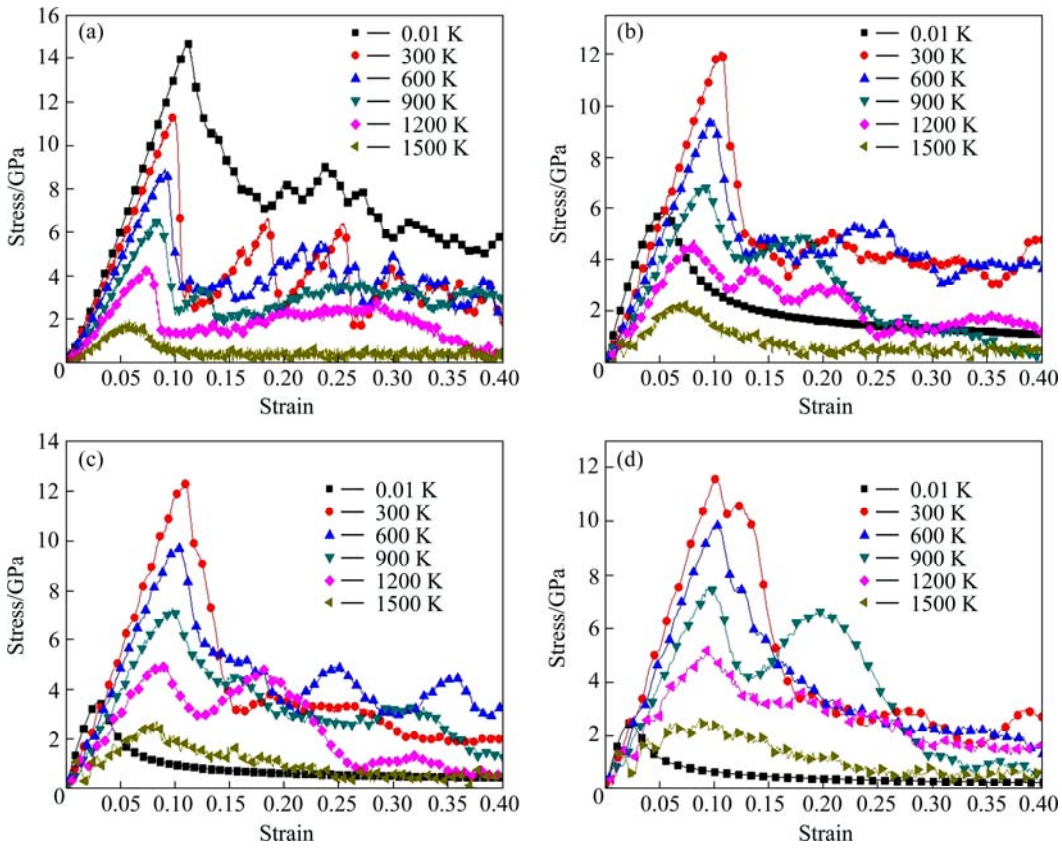

Fig. 3 Stress—strain curves of nickel nanowires with diameters of 4.95 nm at different strain rates of: (a) 1.384×10^{9} s^{-1}; (b) 5.536×10^{9} s^{-1}; (c) 9.688×10^{9} s^{-1}; (d) 1.384×10^{10} s^{-1}

Table 2 Elastic modulus of nickel nanowires at different strain rates and temperatures

Stain rate/s^{-1}	Diameter/nm	Elastic modulus/GPa					
		0.01 K	300 K	600 K	900 K	1200 K	1500 K
1.384×10^{9}	3.94	134.2	116.5	98.6	79.0	57.5	−
	4.95	136.5	119.3	102.5	83.0	64.6	35.0
	5.99	134.7	117.9	102.6	84.5	65.5	38.2
5.536×10^{9}	3.94	−	116.8	98.3	78.0	56.3	−
	4.95	−	119.4	102.1	81.4	61.7	35.5
	5.99	−	117.8	101.9	84.8	65.7	40.3
9.688×10^{9}	3.94	−	116.9	98.8	78.9	57.0	−
	4.95	−	118.9	101.8	81.6	63.6	32.0
	5.99	−	117.1	101.0	84.2	64.4	37.7
1.384×10^{10}	3.94	−	116.4	98.5	77.6	55.3	−
	4.95	−	117.9	101.0	81.2	56.8	33.5
	5.99	−	116.2	100.4	84.2	59.7	35.4

Table 3 Yield strength of nickel nanowires at different strain rates and temperatures

Stain rate/s^{-1}	Diameter/nm	Yield strength/GPa					
		0 K	300 K	600 K	900 K	1200 K	1500 K
1.384×10^{9}	3.94	14.8	11.1	8.5	6.5	4.2	−
	4.95	14.8	11.4	9.0	6.5	4.2	1.8
	5.99	14.5	11.1	8.6	6.5	4.5	2.0
5.536×10^{9}	3.94	5.6	12.0	9.2	6.8	3.8	−
	4.95	5.8	12.1	9.5	6.9	4.7	2.3
	5.99	6.1	11.8	9.0	7.0	4.8	2.5
9.688×10^{9}	3.94	3.5	12.2	9.5	6.7	4.5	−
	4.95	3.5	12.3	9.7	7.1	4.9	2.5
	5.99	3.5	12.0	9.5	7.3	5.0	2.7
1.384×10^{10}	3.94	2.3	11.5	9.5	7.1	5.0	−
	4.95	2.5	11.5	9.9	7.5	5.0	2.5
	5.99	2.6	11.5	9.6	7.4	5.0	2.6

the increasing of temperature. According to the theory of thermodynamics, the total kinetic energy of all the atoms of the system generally satisfies the following equation [30]:

$$E_{\mathrm{k}}=\sum_{i=1}^{N}\frac{1}{2}mv_i^2=\frac{3}{2}Nk_{\mathrm{B}}T \tag{3}$$

where E_{k} is the total kinetic energy of the system; N is the total number of atoms; k_{B} is the Boltzmann constant; T is the thermodynamic temperature.

According to Eq. (3), it can be concluded that the higher the temperature is, the greater the total kinetic energy the system contains, and the faster the atoms move. From the thermodynamic point of view, the thermal motion of the atoms is more intense, which generates greater amplitude in its equilibrium position. Under external loads, the attractive force between atoms relatively reduced and atoms breaks away from the equilibrium position easily, so the stress of the nanowires reduces at the same strain, and elastic modulus decreases.

The yield strength decreases as the temperature increases. According to Eq. (3), the higher the temperature is, the more active the atoms become, and the more easily the atoms escape from their equilibrium position, resulting in lattice defects. Being at the same strain, the lattice defects and crystal dislocation of the nanowires are more intense at higher temperature so that the nanowires are more easily to reach their yielding limits, i.e. yield strengths. Therefore, the yield strengths of the nanowires at higher temperatures will be lower than those at lower temperatures.

From Figs. 3(b)−(d), an unique phenomenon can be found that the yield strengths at 0.01 K are much lower than those at 300 K, which don't follow this law that the higher the temperature is, the lower the yield strengths will become. This phenomenon will be discussed in the next section. It also can be seen from Fig. 3 that the curves are smooth at 0.01 K. As the temperature increases, the curve takes on some certain fluctuation: the higher the temperature is, the more intense the fluctuation becomes. The phenomenon above is due to that high temperature will produce great kinetic energy of the system, which will make it much more difficult to reach a relative steady state for the simulated system.

One can find that the gradients of the stress—strain curves become overall gentle at 1500 K, which is because this temperature is close to the melting point of nickel, and there are a large number of lattice defects inside the nanowires. In another word, the nanowires are at unstable states, and the deformation contributes little to the stress.

The temperature of 1800 K is much higher than the melting point of bulk nickel, which may be consistent with nickel nanowire. That is to say, the nanowires may be in melting stage and the nickel atoms are not in the form of FCC lattice yet.

3.3.2 Dependence on strain rate

It's noted that with the increasing of the strain—rate, the ultrathin nickel nanowire will rupture at a smaller and smaller strain. In another word, the high strain-rate will result in rapidly rupture. According to data listed in Tables 2 and 3, the curves of the elastic moduli and the yield strengths of nanowires versus temperatures can be drawn at different strain rates, as shown in Fig. 4. Figure 4(a) shows these tensile parameters at the lowest strain rate of 1.384×10^9 s^{-1}, and Fig. 4(b) shows those at a higher strain rate of 9.688×10^9 s^{-1}. It's obvious that both elastic modulus and yield strength of different diameter nanowires are basically equal to each other at the same strain rate.

It can be found that there are some differences between the curves in Figs. 4(a) and (b). The curves of both the elastic modulus and the yield strength versus temperatures in Fig. 4(a) have a uniform trend at the lowest strain rate of 1.384×10^9 s^{-1}. However, at other higher strain rates (5.536×10^9, 9.688×10^9 and 1.384×10^{10} s^{-1}), the elastic moduli are not given and the yield strengths are also lower compared to those at other temperatures. According to Fig. 3, the reason for the above phenomenon can be found. At higher strain rate, the stress—strain curves are nonlinear during the elastic stretching process at 0.01 K, so that one uniform value for the elastic modulus can't be obtained.

This phenomenon shows that the yield strengths at

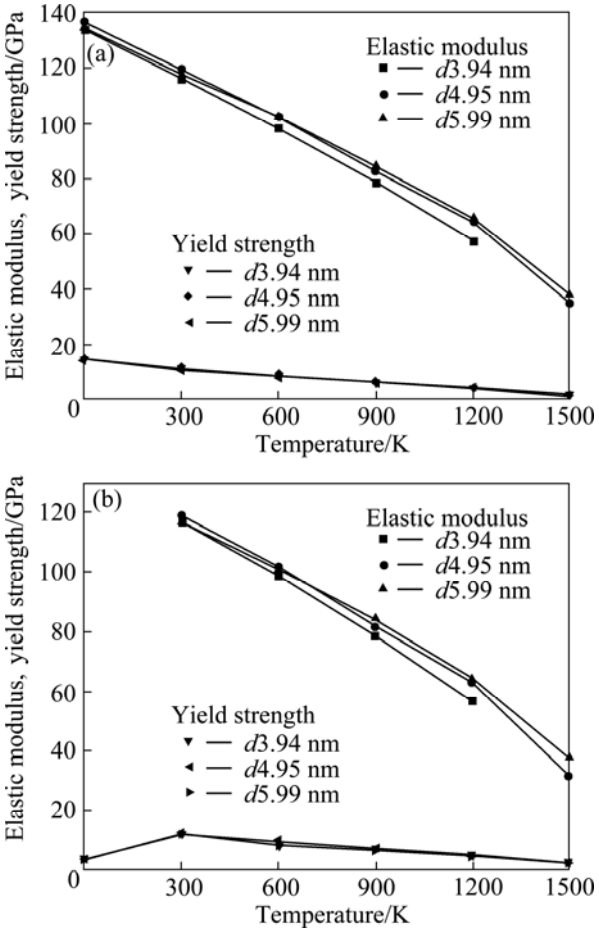

Fig. 4 Elastic modulus and yield strength of nickel nanowires at different strain rates: (a) 1.384×10^9 s^{-1}; (b) 9.688×10^9 s^{-1}

0.01 K are much lower than those at 300 K when the strain rate is relative higher than 1.384×10^9 s^{-1}. At the ideal temperature of 0.01 K, the system kinetic energy is very small, in other words, the nickel atoms are all most in stationary state. If the strain rate is very high during the stretching process, the nickel atoms have not enough time to response the forced movement to get theirs new equilibrium positions. Therefore, comparing with 300 K, the nanowire will step into its yielding state at a relative smaller strain and stress at 0.01 K, producing a large number of lattice detects at both ends of the nanowire. Soon after, the nickel nanowire will go into the brittle fracture state. Figure 5 shows the nanowire morphologies during the stretching process of *d*4.95 nm nickel nanowire at 0.01 K and strain rate of 5.536×10^9 s^{-1}. The brittle fracture occurs at a small strain of 0.089 on both ends of the nanowire, and the majority of the nanowires keeps its initial morphology during the entire stretching process.

Figure 6 shows the stress—strain curves at 0.01 K and at a relatively higher strain rate of 5.536×10^9 s^{-1} for different diameter nickel nanowires. The stress—strain curves are overall smooth and have the same trend at the

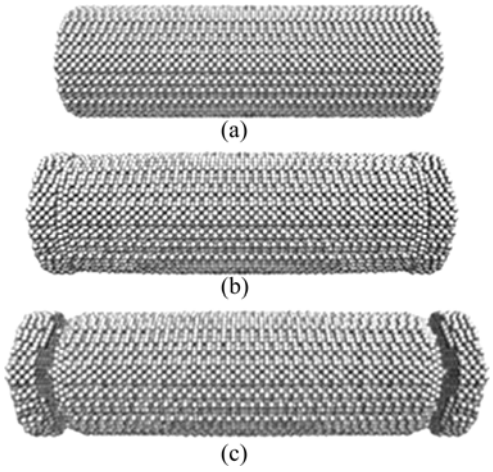

Fig. 5 Morphologies of d4.95 nm nickel nanowire at 0.01 K and strain rate of 5.536×10^{9} s^{-1}: (a) ε=0; (b) ε=0.054; (c) ε=0.089

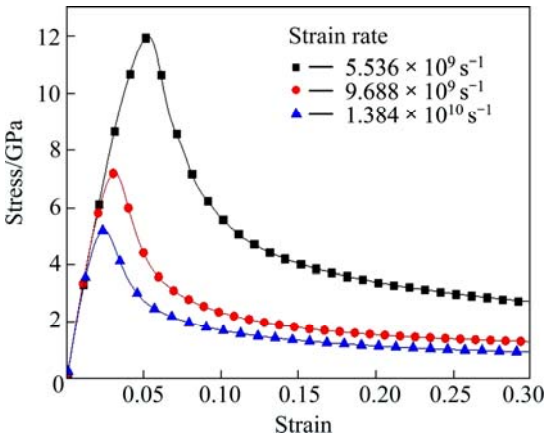

Fig. 6 Stress—strain curves of d5.99 nm nickel nanowires at 0.01 K and at different strain rates

initial stretching stage, but there is almost no linear region during the elastic stretching process. It's obvious that the strain rates have great impacts on yield strength and yield stress. The higher the stress rate is, the lower the yield strength becomes and the small the yield stress is.

Figure 7 shows the stress strain curves of the d3.94 nm nickel nanowire at different strain rates. The curves for other diameter nanowires at other higher temperatures have similar trends. It can be concluded that the strain rate has little effects on the elastic modulus, that is to say, at 300 K or higher temperatures, the elastic modulus basically maintains one uniform value no matter how large the strain rate is. However, there no apparent regularity with the effects of the strain-rate on the yield strength. From Table 3, it can be found that the yield strengths at the same temperature except for 0.01 K don't differ much at all.

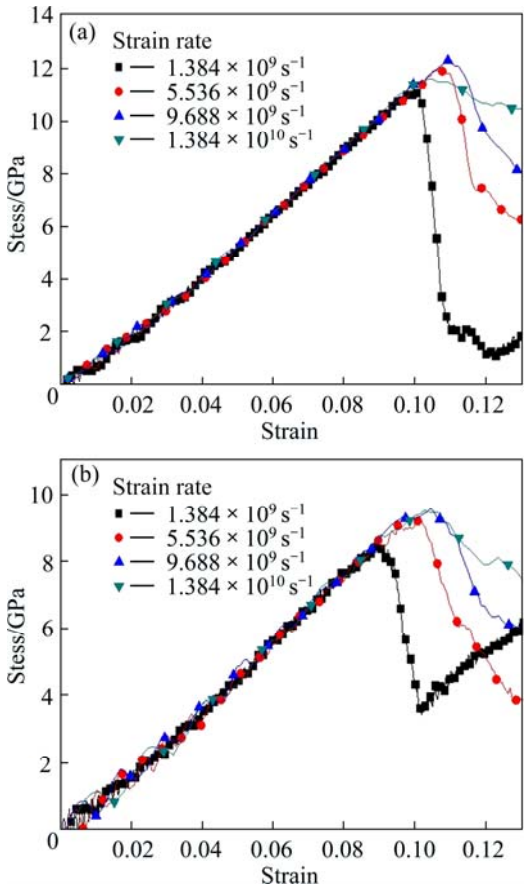

Fig. 7 Stress—strain curves of d3.94 nm nickel nanowire at 300 K (a) and 600 K (b) at different strain rates

3.3.3 Size effects on tensile properties

Figure 8 compares the stress—strain curves of nickel nanowires with different diameters at 300 K and strain rate of 1.384×10^{9} s^{-1}. It should be noted that at other given temperature and strain rate, the similar trend will happen to the stress—strain curves of the ultrathin nanowires with different diameters.

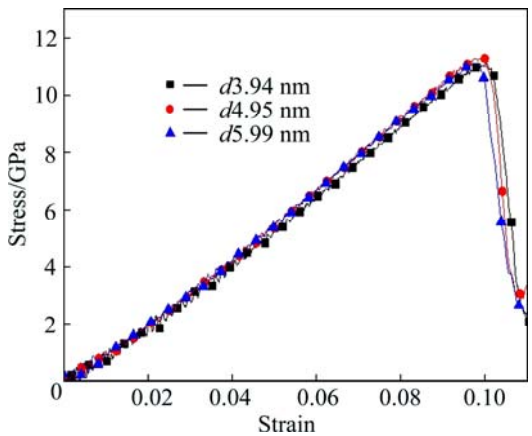

Fig. 8 Stress—strain curves of nickel nanowires with different diameters at 300 K and at strain rate of 1.384×10^{9}

From Fig. 8 and Table 2, one can find that the elastic modulus of the *d*3.94 nm nanowire is a little less than those of the *d*4.95 nm and *d*5.99 nm nanowires. Here, the length-diameter ratio defined by the ratio between length and diameter of the nanowire is adopted to explain this phenomenon. For ultrathin nanowires, the larger the length-diameter ratio is, the poorer stability the nanowire will become.

In addition, the smaller diameter nanowires have relatively larger specific surface area, and the lattice defects mainly occur on the surface of the nanowires, which makes the smaller diameter nanowires have the higher ratio of lattice defects to all of the lattice structures of the simulated system. The degree of lattice defects of the nanowires directly affects the elastic modulus of nanowires, so the *d*3.94 nm nanowire has the lowest elastic modulus at the same strain rate. If the diameter is further reduced, the nanowire would not even stay steady.

The stress—strain curves of *d*3.94 nm nanowires could not be obtained at temperature of 1500 K in Fig. 4, hence there are no elastic modulus and yield strengths for the *d*3.94 nm nanowires. At 1500 K, the nickel atoms move faster than those at other lower temperatures, which may result in much more lattice defects in the *d*3.94 nm nanowire. Also the stretching process makes the lattice defects more serious, which leads to the greatly poor stability. Therefore, during the stretching process, the *d*3.94 nm nanowires cannot exist stably although 1500 K is lower than the melting point.

4 Conclusions

1) Under constant temperature, the stress—strain curves of nickel nanowires show substantially linear relationships during the early stretching process; once exceeding the yield strengths, the stresses of nickel nanowires reduce quickly.

2) The temperature dependence and the strain rate dependence on tensile properties of nickel nanowires are respectively discussed. Elastic modulus and yield strength are gradually decreasing with the increase of temperature. At 0.01 K, the yield strength of the nanowires drops rapidly with the strain rate increasing, and at other temperature the strain rate has little influence on the elastic modulus and the yield strength. At 1500 K, the nickel nanowire with the smallest diameter of *d*3.94 nm could not remain in a stable state during the stretching processes. Because 1800 K exceeds the melting point of nickel nanowires, all of the ultrathin nickel nanowires could not exist at 1800 K.

References

[1] CADEMARTIRI L, OZIN G A. Ultrathin nanowires—A materials chemistry perspective [J]. Advanced Materials, 2009, 21(9): 1013−1020.

[2] ZENG W, MIAO B, LIN L, XIE J. Facile synthesis of NiO nanowires and their gas sensing performance [J]. Transaction of Nonferrous Metals Society of China, 2012, 22(S1): s100−s104.

[3] GLEITER H. Nanostructured materials: Basic concepts and microstructure [J]. Acta Mater, 2000, 48(1): 1−29.

[4] LU L, SHEN Y, CHEN X, QIAN L, LU K. Ultrahigh strength and high electrical conductivity in copper [J]. Science, 2004, 304(5669): 422−426.

[5] WU H A. Molecular dynamics study on mechanics of metal nanowire [J]. Mechanics Research Communications, 2006, 33(1): 9−16.

[6] WU H A, SOH A K, WANG X X, SUN Z H. Strength and fracture of single crystal metal nanowire [J]. Key Engineering Materials, 2004, 261−263: 33−38.

[7] DIAO J, GALL K, DUNN M. Yield strength asymmetry in metal nanowires [J]. Nano Letters, 2004, 4(10): 1863−1867.

[8] GALL K, DIAO J, DUNN M L. The strength of gold nanowires [J]. Nano Letters, 2004, 4(12): 2431−2436.

[9] PARK H S, GALL K, ZIMMERMAN J A. Shape memory and pseudo elasticity in metal nanowires [J]. Physical Review Letters, 2005, 95(25): 255504.

[10] PARK H S, ZIMMERMAN J A. Stable nanobridge formation in (110) gold nanowires under tensile deformation [J]. Scripta Materialia, 2006, 54(6): 1127−1132.

[11] LIANG W, ZHOU M. Atomistic simulations reveal shape memory of FCC metal nanowires [J]. Physical Review, 2006, 73(11): 115409.

[12] KOH S J A, LEE H P, LU C, CHENG Q H. Molecular dynamics simulation of a solid platinum nanowire under uniaxial tensile strain: Temperature and strain-rate effects [J]. Physical Review, 2005, 72(8): 5414.

[13] PARK H S, GALL K, ZIMMERMAN J A. Deformation of FCC nanowires by twinning and slip [J]. Journal of the Mechanics and Physics of Solids, 2006, 54(9): 1862−1881.

[14] ZHANG H, GU X, ZHANG X, YE X, Gong X. Structures and properties of Ni nanowires [J]. Physics Letters A, 2004, 331(5): 332−336.

[15] ZHANG H, TENG Y, LI S, ZENG X. Study on the structures and properties of Ni nanowires [J]. Journal of Atomic and Molecular Physics, 2007, 24(5): 1045−1048. (in Chinese)

[16] GARCÍA-MOCHALES P, PAREDES R, PELÁEZ S, SERENA P A. The formation of pentagonal Ni nanowires: Dependence on the stretching direction and the temperature [J]. Physica Status Solidi A, 2008, 205(6): 1317−1323.

[17] GARCÍA-MOCHALES P, PAREDES R, PELÁEZ S, SERENA P A. Statistical analysis of Ni nanowires breaking processes: A numerical simulation study [J]. Nanotechnology, 2008, 19(22): 225704.

[18] SETOODEH A R, ATTARIANI H, KHOSROWNEJAD M. Nickel nanowires under uniaxial loads: A molecular dynamics simulation study [J]. Computational Materials Science, 2008, 44(2): 378−384.

[19] HUANG D, ZHANG Q, QIAO P. Molecular dynamics evaluation of strain-rate and size effects on mechanical properties of FCC nickel nanowires [J]. Computational Materials Science, 2011, 50: 903−910.

[20] WEN Y, ZHU Z, SHAO G, ZHU R. The uniaxial tensile deformation of Ni nanowire: Atomic-scale computer simulations [J]. Physica E: Low-dimensional Systems and Nanostructures, 2005, 27(1−2): 113−120.

[21] WEN Y, ZHU Z, ZHU R. Molecular dynamics study of the mechanical behavior of nickel nanowire: Strain rate effects [J]. Computational Materials Science, 2008, 41(4): 553−560.

[22] SANSOZ F, DUPONT V. Nanoindentation and plasticity in nanocrystalline Ni nanowires: A case study in size effect mitigation [J]. Scripta Materialia, 2010, 63(11): 1136−1139.

[23] ZHENG H, CAO A, WEINBERGER C R, HUANG J Y, DU K, WANG J, MA Y, XIA Y, MAO S X. Discrete plasticity in sub-10-nm-sized gold crystals [J]. Nature Communications, 2010, 1(144): 1−8.

[24] LU Y, SONG J, HUANG J Y, LOU J. Surface dislocation nucleation mediated deformation and ultrahigh strength in Sub-10-nm Gold nanowires [J]. Nano Research, 2011, 4(12): 1261−1267.

[25] LU Y, SONG J, HUANG J Y, LOU J, Fracture of Sub-20nm ultrathin gold nanowires [J]. Advanced Functional Materials, 2011, 21(20): 3982−3989.

[26] KANG K, CAI W. Size and temperature effects on the fracture mechanisms of silicon nanowires: Molecular dynamics simulations [J]. International Journal of Plasticity, 2010, 26(9): 1387−1401.

[27] DAW M S, BASKES M I. Quantum mechanical calculation of hydrogen embrittlement in metals [J]. Physical Review Letters, 1983, 50(17): 1285−1288.

[28] DAW M S, BASKES M I. Embedded-atom method: Derivation and application to impurities, surfaces, and other defects in metals [J]. Physical Review B, 1984, 29(12): 6443−6453.

[29] TERSOFF J. Modeling solid-state chemistry: Interatomic potentials for multi component system [J]. Physical Review B, 1989, 39(8): 5566−5568.

超细镍纳米线拉伸性能的温度和应变率相关性的分子动力学研究

王卫东，易成龙，樊康旗

西安电子科技大学 机电工程学院，西安 710071

摘　要：基于 EAM 势，采用分子动力学方法对超细镍纳米线(直径分别为 3.94、4.95 和 5.99 nm)在〈100〉晶向的拉伸性能进行研究，并对其温度相关性和拉伸应变率相关性进行探讨。结果表明：弹性模量和屈服强度随着温度的升高而逐渐降低，并且随着拉伸应变率的增大，应力—应变曲线波动程度变大，超细镍纳米线发生断裂时的应变越来越小。在 0.01 K 温度下，超细镍纳米线屈服强度随拉伸应变率的升高迅速降低；但在其它温度条件下，拉伸应变率对弹性模量和屈服强度的影响较小。简要分析尺寸大小对镍纳米线拉伸性能的影响。

关键词：超细镍纳米线；温度相关性；应变率相关性；拉伸性能；分子动力学模拟

(Edited by Chao WANG)